



RESEARCH ARTICLE

10.1002/2015GC006110

Key Points:

- M_w 6.2 earthquake due to normal slip on a major preexisting east-dipping rift border fault
- Diking could promote faulting on border faults of the rift in the central part of Lake Kivu
- Diking plays a major role in accommodating upper crustal extension in a considered magma-poor rift

Supporting Information:

- Supporting Information S1
- Supporting Information S2

Correspondence to:

C. Wauthier,
cuw25@psu.edu

Citation:

Wauthier, C., B. Smets, and D. Keir (2015), Diking-induced moderate-magnitude earthquakes on a youthful rift border fault: The 2002 Nyiragongo-Kalehe sequence, D.R. Congo, *Geochem. Geophys. Geosyst.*, 16, doi:10.1002/2015GC006110.

Received 21 SEP 2015

Accepted 16 NOV 2015

Accepted article online 20 NOV 2015

© 2015. The Authors. *Geochemistry, Geophysics, Geosystems* published by Wiley Periodicals, Inc. on behalf of American Geophysical Union.

This is an open access article under the terms of the Creative Commons Attribution-NonCommercial-NoDerivs License, which permits use and distribution in any medium, provided the original work is properly cited, the use is non-commercial and no modifications or adaptations are made.

Diking-induced moderate-magnitude earthquakes on a youthful rift border fault: The 2002 Nyiragongo-Kalehe sequence, D.R. Congo

C. Wauthier^{1,2}, B. Smets^{3,4,5}, and D. Keir⁶

¹Department of Geosciences, Pennsylvania State University, State College, Pennsylvania, USA, ²Institute for CyberScience, Pennsylvania State University, State College, Pennsylvania, USA, ³European Center for Geodynamics and Seismology, Walferdange, Luxembourg, ⁴Department of Geography, Earth System Science, Vrije Universiteit Brussel, Brussels, Belgium, ⁵Earth Sciences Department, Royal Museum for Central Africa, Tervuren, Belgium, ⁶National Oceanography Centre Southampton, University of Southampton, Southampton, UK

Abstract On 24 October 2002, M_w 6.2 earthquake occurred in the central part of the Lake Kivu basin, Western Branch of the East African Rift. This is the largest event recorded in the Lake Kivu area since 1900. An integrated analysis of radar interferometry (InSAR), seismic and geological data, demonstrates that the earthquake occurred due to normal-slip motion on a major preexisting east-dipping rift border fault. A Coulomb stress analysis suggests that diking events, such as the January 2002 dike intrusion, could promote faulting on the western border faults of the rift in the central part of Lake Kivu. We thus interpret that dike-induced stress changes can cause moderate to large-magnitude earthquakes on major border faults during continental rifting. Continental extension processes appear complex in the Lake Kivu basin, requiring the use of a hybrid model of strain accommodation and partitioning in the East African Rift.

1. Introduction

When a continental rift such as the East African Rift System (EARS) evolves toward continental breakup, magma-driven processes, and in particular diking, play an increasingly important role in crustal strain accommodation [e.g., *Ebinger*, 2005; *Keir*, 2014]. Hence, in the more evolved northern region of the East African Rift System (EARS) and in Afar, around 80% of the extension is accommodated by magmatism [e.g., *Bilham et al.*, 1999; *Wright et al.*, 2006]. As a result, magma-driven processes establish and maintain along-axis rift segmentation during continental breakup [*Wright et al.*, 2012] whereas fault-controlled processes, i.e., rift border faults, become inactive [e.g., *Buck*, 2004; *Ebinger*, 2005].

In the Western and Eastern Branches of the EARS which encircle the Tanzanian craton (Figure 1), the continental breakup is in an earlier stage of development and the crust is less extended than in Afar [*Ebinger*, 1989b]. In those two branches, well-developed border faults and rift valley volcanoes are visible, but developed magmatic segments are lacking. Recent geophysical and geological studies of the southern edge of the Eastern Branch in Tanzania indicate that fault-controlled and magma-assisted extensions [*Calais et al.*, 2008; *Baer et al.*, 2008; *Biggs et al.*, 2009, 2013; *Albaric et al.*, 2014] coexist in this weakly extended portion of the EARS. However, the exact contribution, as well as along-rift variations, of strain partitioning between faulting and magmatism remain poorly documented, especially in portions of the EARS which have not been affected by significant amount of crustal thinning.

In contrast to the widespread volcanism observed in the Eastern Branch, the Western Branch is considered as “magma poor” [*Koptev et al.*, 2015] with magmatism only within a limited number and spatially restricted volcanic provinces (e.g., Virunga and South Kivu Volcanic Provinces). Rifting in the Western Branch has started before (~12–7 Ma) [e.g., *Ebinger*, 2005; *Muirhead et al.*, 2015] or coincidentally (~25 Ma) [*Roberts et al.*, 2012] with rifting in the Kenya Rift and further north in the Eastern Branch. Surface geology suggests that significant amounts of extension should be accommodated by magmatism in the Eastern Branch, and by brittle deformation along normal faults in the Western Branch [*Parsons and Thompson*, 1991; *Koptev et al.*, 2015].

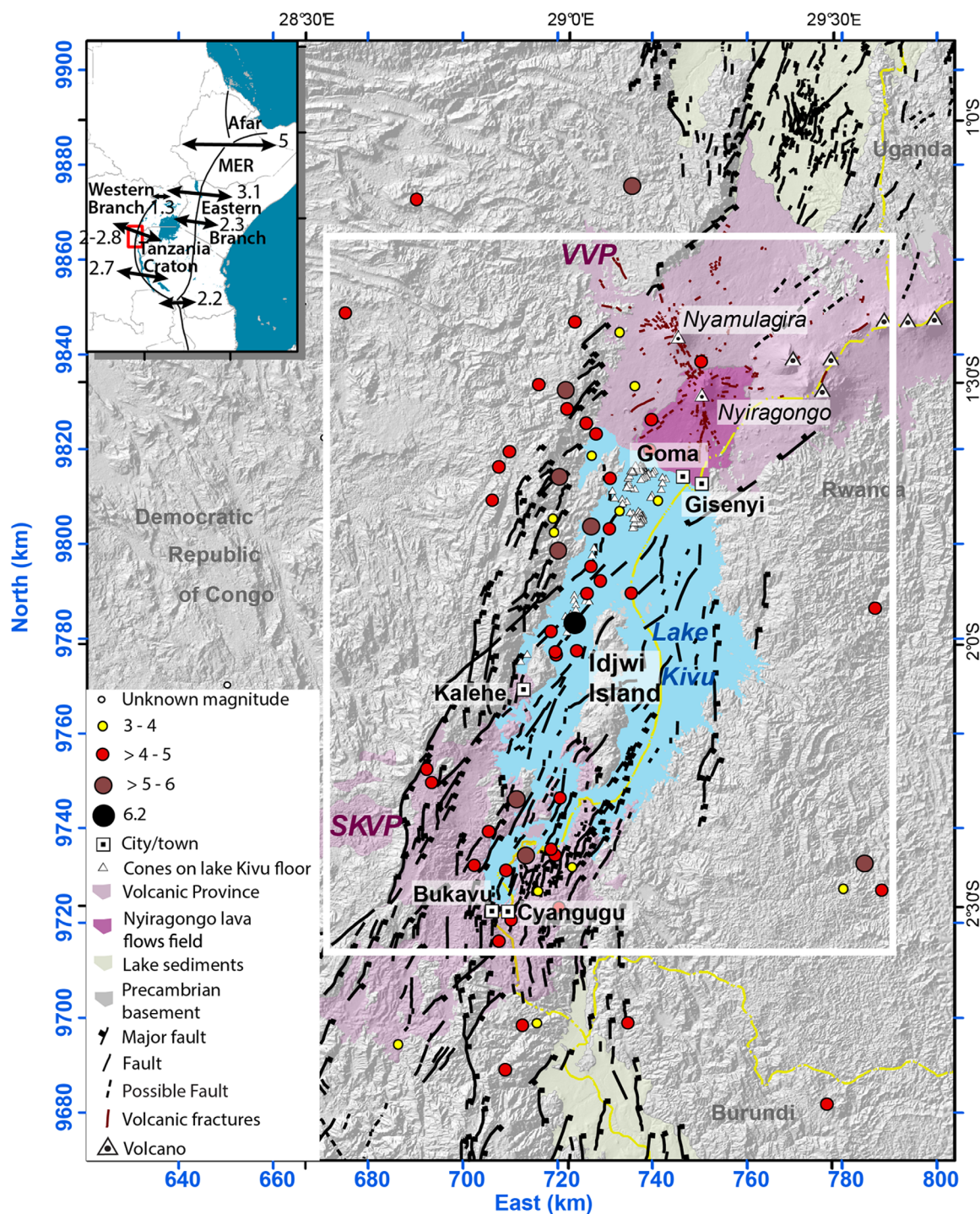


Figure 1. Shaded relief topographic map of the Kivu basin. SKVP and VVP stand for South Kivu Volcanic and Virunga Volcanic Province, respectively. MER stands for Main Ethiopian Rift. The Ruzizi River corresponds to the boundary (yellow line) between the Democratic Republic of Congo and Rwanda, then between Congo and Burundi to the south. Mapped faults are from Smets et al. (submitted manuscript). Earthquakes for the period 1996–2010 are shown (source: NEIC). The earthquakes in the Kivu basin tend to mostly concentrate along western border faults. It is important to note that the earthquakes hypocenters are poorly constrained, the depth being generally fixed to 10 km for shallow events, and the horizontal error estimate being ~10–15 km (source: NEIC). The white outline shows the extent of Figure 2. Top-left inset: arrows show extension direction with numbers representing velocities in mm/yr [Stamps et al., 2008; Saria et al., 2014]. The rift extension direction in the Kivu area is ~N110E with a rate of ~2–2.8 mm/yr [Stamps et al., 2008; Saria et al., 2014].

Pure tectonic extensional-faulting events, consistent with fault-controlled rifts [e.g., McKenzie, 1978; Buck, 2004; Ebinger, 2005], have been observed in the Western Branch using seismic and geodetic data [d'Oreye et al., 2011; Biggs et al., 2010]. Specifically, in the Lake Kivu rift basin, this suggestion was supported by a

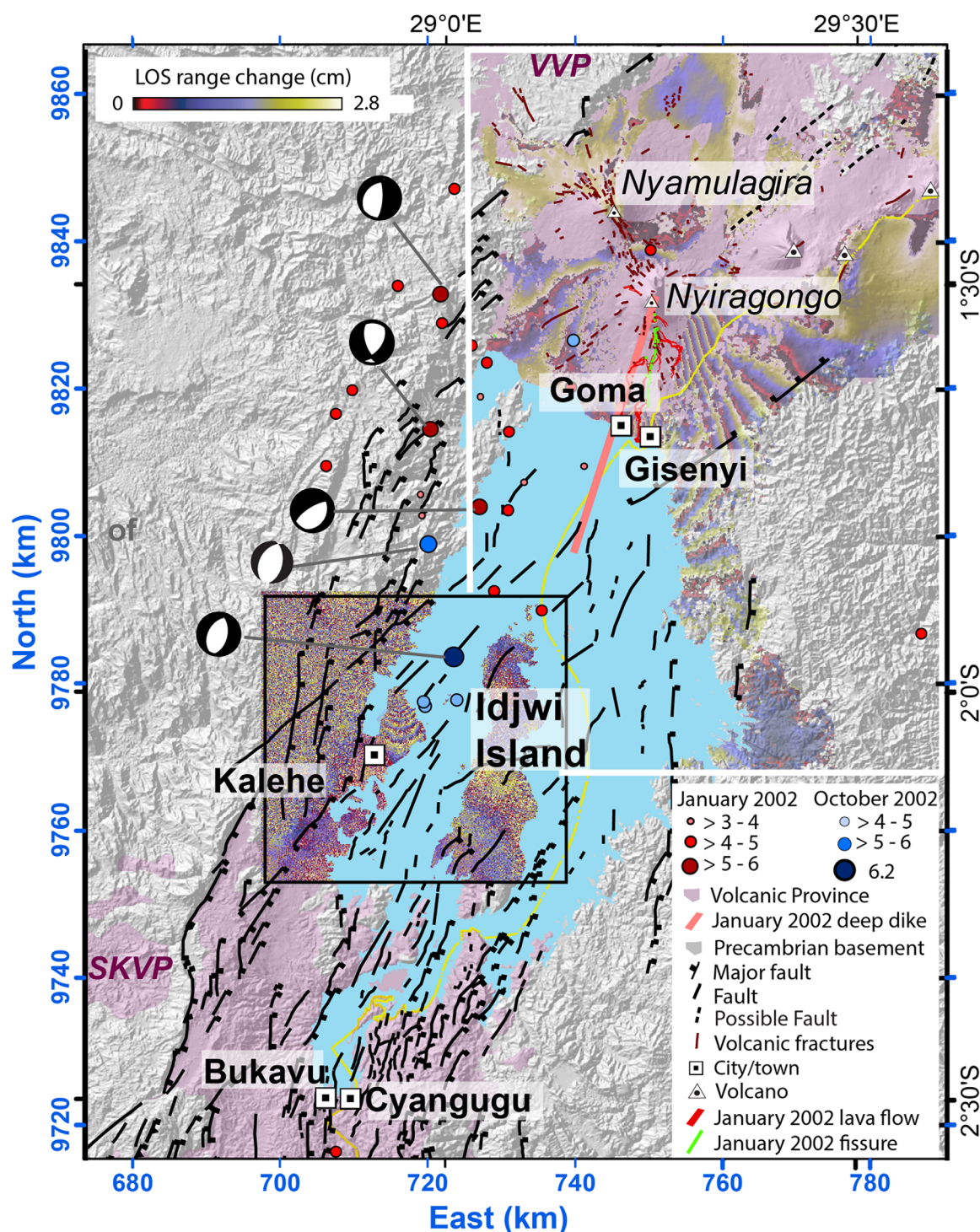


Figure 2. Two wrapped RADARSAT-1 interferograms showing the deformation associated with the 2002 January Nyiragongo eruption (white outline, $H_{amb} = 130$ m, 21 December 2001 to 3 March 2002, Pass = descending) and the 24 October earthquakes (black outline, $H_{amb} = 40$, 5–29 October 2002, Pass = descending). One color cycle (fringe) represents a 2.8 cm line-of-sight range change. Earthquakes for the period January to October 2002 are shown (source: NEIC).

seismic and geodetic study of the Bukavu-Cyangugu M_w 5.9 February 2008 earthquake in the southern part of the Kivu basin [d'Orey et al., 2011] (Figure 1 and supplemental information Table S1). d'Orey et al. [2011] did not infer a magmatic origin for this seismic sequence based on a seismic and geodetic moments budget. However, a recent geodetic study of the Nyiragongo 17 January 2002 eruption suggested strain

accommodation by dike intrusions. The January 2002 dike intrusions created a $\sim 60 \times 60$ km deforming area, north and east of Lake Kivu (Figure 2) and possibly induced secondary faulting in Gisenyi [Wauthier *et al.*, 2012]. The respective roles of fault-controlled versus magma-driven processes in the extension of the Kivu basin are thus being questioned.

In October 2002, RADARSAT-1 satellite images constrained surface deformation associated with the M_w 6.2 Kalehe earthquake, which is the largest earthquake recorded in the Lake Kivu area since 1900 [Mavonga, 2007]. This earthquake occurred on 24 October 2002, at 6:08 UTC in the central part of the Lake Kivu basin, in the Kalehe area (Figure 2). Eight people were killed in the epicentral area of Kalehe and the village was partially inundated by Lake Kivu [Wafula *et al.*, 2007]. To investigate the characteristics and origin of the Kalehe earthquake, we inverted Interferometric Synthetic Aperture Radar (InSAR) data covering the event, and further constrained our models with seismic and structural observations. We performed a Coulomb stress change analysis to test if there is causality between the major diking event in January 2002 and the M_w 6.2 earthquake. This work aims to provide new insights on the potential role of dike intrusion on strain accommodation and partitioning during early stages of continental rifting.

2. Geologic Setting



The Western Branch of the EARS encircling the Archean Tanzania craton (Figure 1) is formed by an en echelon succession of ~ 100 km long and 40–70 km wide grabens and half-graben asymmetric basins often hosting lakes [Rosendhal, 1987; Ebinger, 1989a,b; Ebinger and Furman, 2003]. The asymmetric basins are bound by long border fault systems characterized by up to several kilometers offset [Wood *et al.*, 2015], dipping at angles between 40° and 60° [Zana and Hamaguchi, 1978; Shudofsky, 1985]. Those border faults likely penetrate more than 15 km depth in the crust [Morley, 1989; Yang and Chen, 2010; Craig *et al.*, 2011; d'Oreye *et al.*, 2011; Lindenfeld and Rumpker, 2011].

The Western Branch is thought to have developed in relatively strong and cold lithosphere in which thermal heating and weakening of the upper crust has only been modified by mantle plume and magmatic processes at a few spatially restricted volcanic provinces [Wood *et al.*, 2015]. From north to south, the Western Branch includes four volcanic provinces: Toro-Ankole (Uganda), Virunga (Democratic Republic of Congo, Uganda, Rwanda), South Kivu (Democratic Republic of Congo, Rwanda, Burundi), and Rungwe (Tanzania). They all lie within transfer zones, which are areas accommodating the strain between two distinct rift segments [e.g., Pouclet, 1976, 1977; Ebinger, 1989a,b; Ebinger and Furman, 2003; Corti *et al.*, 2003b].

Lake Kivu is located between the Virunga (VVP) and South Kivu (SKVP) provinces (Figure 1), in which volcanism started ~ 12 and ~ 10 Ma [Ebinger and Furman, 2003], respectively. However, the composite volcanoes of the VVP developed in the past ~ 2.6 Myr, the most recent volcanic activity being concentrated in the center of the rift depression [e.g., Bellon and Pouclet, 1980; Wood *et al.*, 2015]. Nowadays, volcanic activity is almost exclusively restricted to Nyiragongo and Nyamulagira volcanoes (Figure 1), which are the most active African volcanoes [Wright *et al.*, 2015]. Nyamulagira erupts every 1–4 years [Smets *et al.*, 2010] and Nyiragongo, which is usually characterized by intracraternal activity, erupted in two fissural eruptions, likely induced by major dike intrusions, in 1977 [e.g., Tazieff, 1977; Pottier, 1978] and 2002 [e.g., Komorowski *et al.*, 2003; Wauthier *et al.*, 2012]. Both volcanoes currently host a persistent lava lake in their summit crater [Smets *et al.*, 2015].

The Kivu basin is an asymmetric half-graben controlled on its western side by a ~ 110 km long, $\sim N-S$ striking border fault along which most of the seismicity is located (Figure 1). The basin morphology is complex with, in its northern part, a main basin characterized by the underwater extension of the VVP [Ross *et al.*, 2014] and a progressive transfer of the main western rift fault into the lake (B. Smets *et al.*, The role of inherited crustal structures and magmatism in the development of rift segments: Insights from the Kivu basin, western branch of the East African Rift, Tectonophysics, submitted 2015). The central part of the Kivu basin is characterized by two half grabens separated by an uplifted block whose surface expression is the Idjwi Island (Figure 1). To the south, the SKVP marks the southeastward transfer of the rift toward the northern Lake Tanganyika basin [Rosendhal, 1987; Ebinger, 1989b]. The Kivu basin contains up to 1.5 km thickness of sediments [Wong and Von Herzen, 1974; Wood *et al.*, 2015] and basalts derived from the VVP [Ross *et al.*, 2014] and SKVP [Ebinger, 1989b]. Recent offshore multichannel seismic

Table 1. Harvard CMT [Dziewonski *et al.*, 1981; Craig *et al.* 2011] Source Parameters for $M > 5$ Earthquakes in the Lake Kivu Basin Recorded on 24 October 2002^a

Date	Time (UTC)	s1	d1	r1	s2	d2	r2	z (km)	Mw	Moment (e + 18 Nm)	Focal Sphere	Source
24 Oct 2002	6:08	210	42	−75	9	50	−103	15	6.2	2.2		CMT
		209	47	−82				8	6.2			Craig <i>et al.</i> [2011]
24 Oct 2002	7:12	210	42	−75				3	5.5			Craig <i>et al.</i> [2011]

^aStrikes, dips, and rakes of the two nodal planes are s1, d1, and r1 and s2, d2, and r2, and z is the depth.

reflection data [Wood *et al.*, 2015] show no displacement of the upper sediment layers for the eastern border of the Kivu basin. The Kivu basin is narrower and contains a thinner layer of sediments compared to the Albert, Edward, Tanganyika, and northern Malawi rift segments. This observation led Wood *et al.* [2015] to infer that the crust is less extended in the Kivu basin. According to Smets *et al.* (submitted manuscript), the geomorphology of the Kivu basin might be related to normal faulting, magma underplating, and differential erosion. The latest state of the Kivu basin would only date back to 10 kyr, when the lavas of Nyiragongo and Nyamulagira dammed the northward flow of a former hydrographic network, creating the present Lake Kivu and forcing the waters to flow through the Ruzizi River to the south, toward Lake Tanganyika [e.g., Peeters, 1957; Ross *et al.*, 2014; Wood *et al.*, 2015; Smets *et al.*, submitted manuscript]. On the basis that the flank elevation varies along strike, the narrowness of the basin, the presence of several large volcanic edifices within the central rift, as well as magma underplating and intrusion, Wood *et al.* [2015] suggest that the southern part of lake Kivu basin experienced less subsidence and likely less crustal extension than the central and northern parts of the Kivu basin.

3. Seismic and Geodetic Data

Constraints on the Kalehe earthquakes are provided by global seismic stations with locations of 30 earthquakes in 2002 provided by the USGS/NEIC catalog (supplemental information Table S1) and moment tensor inversion performed on two earthquakes by Craig *et al.* [2011] (Table 1). These data show that the 24 October 2002 M_w 6.2 earthquake has a normal fault-type focal mechanism (Figure 2 and Table 1). Figure 3a shows the estimated epicenter for the main shock and the four major recorded aftershocks (supplemental information Table S1), the strongest of which occurred about 1 h after the main shock at 07:13 with a M_w 5.5 [Mavonga, 2007; Midzi and Manzunzu, 2014; Craig *et al.*, 2011] and a similar normal fault-type focal mechanism (Table 1). We add additional constraints on the temporal evolution of the sequence using the continuous seismic record from the nearest permanent seismic station to Kivu (supplemental information Figure S1, MBAR located ~ 250 km from the main shock) during October 2002. During 5–29 October 2002, we compute local magnitude (M_L) of 88 well-recorded earthquakes in the sequence, with the catalog magnitude of completeness of 4.1 and a b-value of 0.9 (supplemental information Figure S2). The total cumulative seismic moment (M_o) release is estimated to be 4.75×10^{18} Nm (Figure 3d). Using a local network, Mavonga [2007] reported a total of 326 earthquakes associated with the Kalehe sequence, with an aftershock distribution extending to Idjwi Island. However, the fault plane is not visible since the aftershocks are reported by Mavonga [2007] to have an elliptical distribution.

InSAR data provide the only geodetic measurement of the earthquake. A RADARSAT-1 descending interferogram (5 October 2002 to 29 October 2002) imaged the event (Figures 2 and 3). The interferogram was processed using the JPL/Caltech ROI_PAC SAR software, multilooked with a factor of 2 in range and azimuth and filtered with an adaptive filter to optimize the signal-to-noise ratio [Rosen *et al.*, 2004]. We removed the orbital and topographic interferometric phase contribution using precise orbits and a 30 m resolution digital elevation model generated by the NASA Shuttle Radar Topography Mission [Farr *et al.*, 2007]. The interferometric phase has been unwrapped with the SNAPHU algorithm [Chen and Zebker, 2001]. Despite the sparseness of the data, due to the vegetation-induced temporal decorrelation and the presence of the lake, seven clear fringes indicating a range increase of ~ 20 cm are visible on the western lake shore in the Kalehe area (Figure 3a). They are consistent with ground subsidence of the Kalehe area associated with normal faulting.

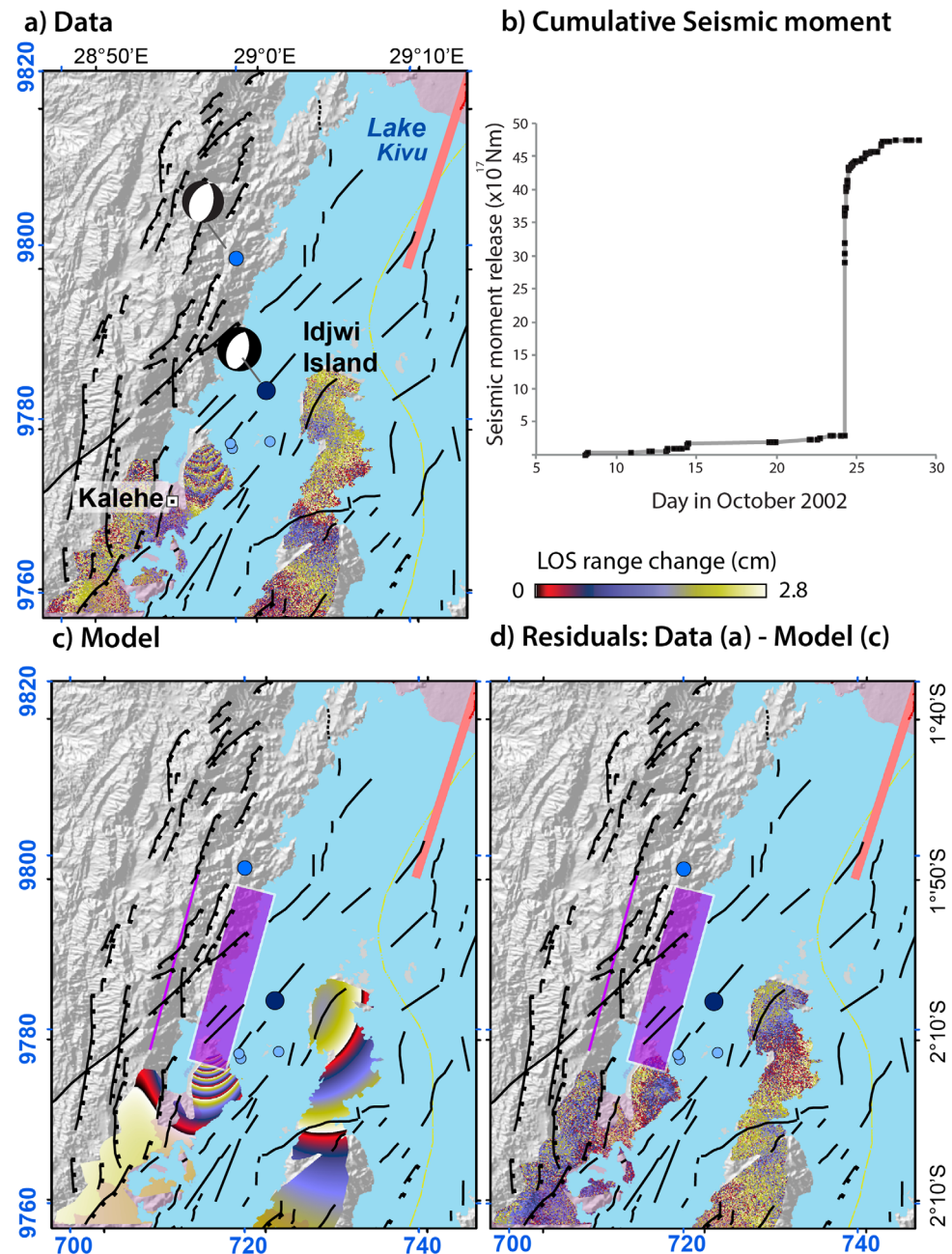


Figure 3. (a) InSAR data and the earthquakes for the period 5 October 2002 to 29 October 2002 are shown in shades of blue (source: NEIC). (b) Cumulative seismic moment release during the same period associated with the Kalehe earthquake swarm estimated from the 88 earthquakes recorded at station MBAR. The majority of seismic moment release occurred during the mainshock at 06:09 24 October and the largest aftershock at 07:13 24 October. (c) Geodetic model and (d) residuals for uniform slip inversions for the 2002 Kalehe earthquake. The fault area projection is shown in purple outlined in white, while the fault trace corresponding to the prolongation of the fault to the surface is the purple line.

4. Results

4.1. Geodetic Modeling

Given the limited InSAR data set, we used simple modeling methods providing an analytical solution in an elastic half-space to model the geodetic data. Specifically, a rectangular dislocation with uniform rake [Okada, 1985] describes the fault rupture. The value of the Poisson ratio and Young modulus is assumed to be 0.25 and 90 GPa (supplemental information Figure S4), respectively.

Table 2. Best Fit Parameters for the Four Tested Models Given With Their 95% Confidence Intervals Following *Sambridge* [1999b]^a

Model Orientation	1 W-dipping nodal plane	2 W-dipping nodal plane	3 E-dipping nodal plane	4** E-dipping nodal plane
Strike (°)	200 ^[200 203]	205 ^[203 208]	4 ^[0 11]	15 ^[12 19]
Dip (°)	49 ^[47 52]	41 ^[37 45]	40 ^[40 45]	40 ^[40 44]
Rake (°)	−69 ^[−69 −65]	−78 ^[−84 −70]	−106 ^[−108 −97]	−93 ^[−98 −93]
Slip (m)	1 ^[0.3 1]	0.7 ^[0.4 1.8]	1.7 ^[1.2 2]	1.3 ^[0.3 1.8]
Length (km)	30 ^[27 30]	21 ^[18 22]	29 ^[22 30]	21 ^[19 22]
Width (km)	11 ^[10 12]	10 ^[10 16]	10 ^[10 13]	6 ^[6 8]
Min. Depth (km)	5*	4*	5*	4*
Max. Depth (km)	13 ^[9 15]	14 ^[12 17]	11 ^[9 13]	8 ^[5 10]
RMS error (mm)	7.5	7.6	7.9	6.9
East (km)	725 ^[720 729]	725 ^[721 728]	708 ^[708 710]	712 ^[711 715]
North (km)	9788 ^[9784 9790]	9783 ^[9778 9786]	9791 ^[9787 9793]	9788 ^[9785 9792]
Moment (e + 18 Nm)	13.9 ^[3 14]	7.8 ^[2.6 23]	17.5 ^[9.5 28]	5.9 ^[1.2 11]

^a* and ** denote a parameter which was fixed during inversions and the preferred best fit model, respectively.

To infer the geometry and rake of the fault that created the observed deformation field, we inverted the subsampled RADARSAT-1 data set with a near-neighborhood algorithm [*Sambridge*, 1999a]. The misfit function quantifying discrepancy between observed and modeled displacements is defined as:

$$\chi^2 = (\mathbf{u}_0 - \mathbf{u}_c)^T \mathbf{C}_d^{-1} (\mathbf{u}_0 - \mathbf{u}_c) \quad (1)$$

where \mathbf{C}_d is the data covariance matrix and \mathbf{u}_0 and \mathbf{u}_c are vectors of subsampled observed and modeled line-of-sight displacements, respectively. We also use a more intuitive indicator to compare inversions results, an *RMS error*, defined as:

$$RMS = \left(\sqrt{\frac{(\mathbf{u}_0 - \mathbf{u}_c)^T (\mathbf{u}_0 - \mathbf{u}_c)}{N}} \right) \quad (2)$$

where N is the number of subsampled data points.

The 95% confidence intervals on best fit parameters are calculated during an appraisal stage following *Sambridge* [1999b] and *Fukushima et al.* [2005]. Note that from synthetic tests, *Dawson and Tregoning* [2007] inferred that fault source parameters are found to be accurately determined from one SAR viewing geometry.

The two nodal plane solutions identified from the seismic moment tensor solution [*Craig et al.*, 2011] (see Table 1) served as guides for the inversions. In the inversions, the search intervals for the fault rake, dip, and strike angles parameters consider a range of $\pm 10^\circ$ from the nodal plane solutions. The search intervals for the length and width of the fault plane consider a range of ± 5 km from: (1) a rectangular fault plane of $\sim 16 \times 11$ km, based on the *Wells and Coppersmith* [1994] scaling laws, and (2) a rectangular fault plane of $\sim 25 \times 15$ km, based on *Mavonga* [2007]. Finally, the hypocenter depth is inverted between the surface and 15 km depth.

All four best fitting models obtained for each tested case fit the geodetic and seismic data satisfactorily (supplemental information Figure S3). However, Models 1 and 3, in which the fault geometry was constrained following the larger area estimates (25×15 km) from *Mavonga* [2007], overestimate the seismic moment by a factor 2–3 (Table 2). The preferred best fit model, which includes normal slip on a \sim N15E-trending fault, is Model 4, which has a RMS error of 6.9 mm (Table 2 and Figure 3b). The modeled fault is ~ 21 km long and 6 km wide. Note that the discrepancy in horizontal location between the earthquakes (source: NEIC) and the modeled fault likely results from the ~ 10 – 15 km horizontal error on earthquake locations [e.g., *Hellfrich*, 1997]. The fault extends from a depth of ~ 4 to 8 km below the surface, which is consistent with the main shock and largest aftershock recalculated hypocenters (Table 1) [*Craig et al.*, 2011]. The modeled fault rake is -93° which corresponds to normal slip in a \sim N57E direction. The total geodetic moment of 5×10^{18} Nm is in close agreement with the total seismic moment of 4.75×10^{18} Nm released during 5–29 October 2002 (Figure 3).

4.2. Stress Transfer

To test whether the modeled deep January 2002 dike intrusion could have triggered the subsequent seismicity in the Kalehe area, we calculate Coulomb stress changes induced by the intrusion [Wauthier *et al.*, 2012] on receiver faults corresponding to the best fit geodetic fault model (Model 4 in Table 2).

The Coulomb failure hypothesis is:

$$\Delta\sigma_{\text{Coulomb}} = \Delta\tau + \mu' \Delta\sigma_n \quad (3)$$

Failure is promoted when $\Delta\sigma_{\text{Coulomb}}$ on the receiver fault caused by opening and/or slip on the source dislocation increases. $\Delta\tau$ is the shear stress change (positive in the direction of receiver fault slip), $\Delta\sigma_n$ is normal stress change (positive when the receiver fault is unclamped), and μ' is the effective fault friction coefficient on the receiver fault. We used the Coulomb 3-D software [Toda *et al.*, 2011] and assumed a Poisson's ratio and effective fault friction coefficient of 0.25 and 0.4, respectively. Considering the depth-dependent rigidity estimated for this area [Mavonga, 2010; Wauthier *et al.*, 2012], we assume a Young's modulus of 90 GPa (supplemental information Figure S4).

Wauthier *et al.* [2012] constrained the extent of a deep dike intrusion beneath Lake Kivu, and in particular, the southern dike tip, thanks to the deformation pattern imaged by RADARSAT-1 data sets coherent on the eastern shore of the lake. This dike is used as the dislocation source for the Coulomb stress calculation. For simplicity, we approximated the deep dike source geometry inferred by Wauthier *et al.* [2012] with a single rectangular dislocation whose top is at ~ 3 km depth, height is ~ 6 km for a length of ~ 35 km, and affected by a mean opening of ~ 0.72 m. Note that to test the robustness of our results, upper and lower limits of the dike extent and crustal rigidities have also been tested (supplemental information Figures S5 and S6). In all cases, the October 2002 earthquake hypocenters and the best fit modeled fault are located in regions of positive Coulomb stress change (Figure 4 and supplemental information Figures S5 and S6). Coulomb stress are increased on the receiver fault plane corresponding to the best fit geodetic model for the Kalehe earthquake by a maximum of ~ 0.4 bar (Figure 4). These results suggest that the major January 2002 dike intrusion brought faults closer to failure and unclamped the Kalehe area.

5. Discussion

The modeled fault surface trace projection is consistent with $\sim N15E$ oriented en-echelon east-dipping normal faults visible at the surface correspond to major active [Wood *et al.*, 2015] rift escarpments (Smets *et al.*, submitted manuscript; Figure 3b). Therefore, we infer that the preferred modeled fault related to the M_w 6.2 Kalehe earthquake corresponds to the first nodal plane of the moment tensor solution, which is oriented $\sim N15E$ and dips eastward. Note that $\sim N45E$ oriented faults crossing the $\sim N15E$ main rift escarpments faults correspond to a secondary faulting axis in the Kivu area, likely following preexisting Precambrian structures [Villeneuve, 1980]. The fault also strikes parallel to the January 2002 dike. The similar orientation, parallel to the local rift axis for both structures, indicates that this direction is guided uniquely by the rift extension.

Magmatic activity can trigger moderate-magnitude earthquakes on suitably oriented preexisting faults [e.g., Walter and Amelung, 2006; Yokoyama, 2001; Toda *et al.*, 2002; Hayashi and Morita, 2003; Nishimura *et al.*, 2001; Wauthier *et al.*, 2013]. Injection of the January 2002 Nyiragongo deep dike has hence likely triggered post-eruptive seismicity [Kavotha *et al.*, 2003], as well as three other $M > 5$ earthquakes in January 2002 (supplemental information Table S2 and Figure S4). Furthermore, Passarelli *et al.* [2015] found that dike-induced strike-slip events that follow the Gutenberg-Richter model (b -value ~ 1) occurred on suitably oriented preexisting tectonic structures. Therefore, we suggest that the January 2002 dike intrusion induced the largest magnitude earthquake recorded in the Lake Kivu area on 24 October 2002, along suitably oriented preexisting rift structures. The maximum Coulomb stress change does not exceed 1 bar, but it is likely that other similar diking events such as in 1977 [Tazieff, 1977] also accumulated stress on the western rift border faults in the central part of Lake Kivu. Three $\sim M5$ earthquakes (source: NEIC) indeed occurred following the 10 January 1977 eruption and the related dike intrusion, two were located in the Bukavu area and one on the western side of Lake Kivu. However, note that diking events below Nyiragongo and Goma with a similar southern extension than this one are unlikely to significantly modify the stress field in the southernmost part of the Lake Kivu including the SKVP and Bukavu areas.

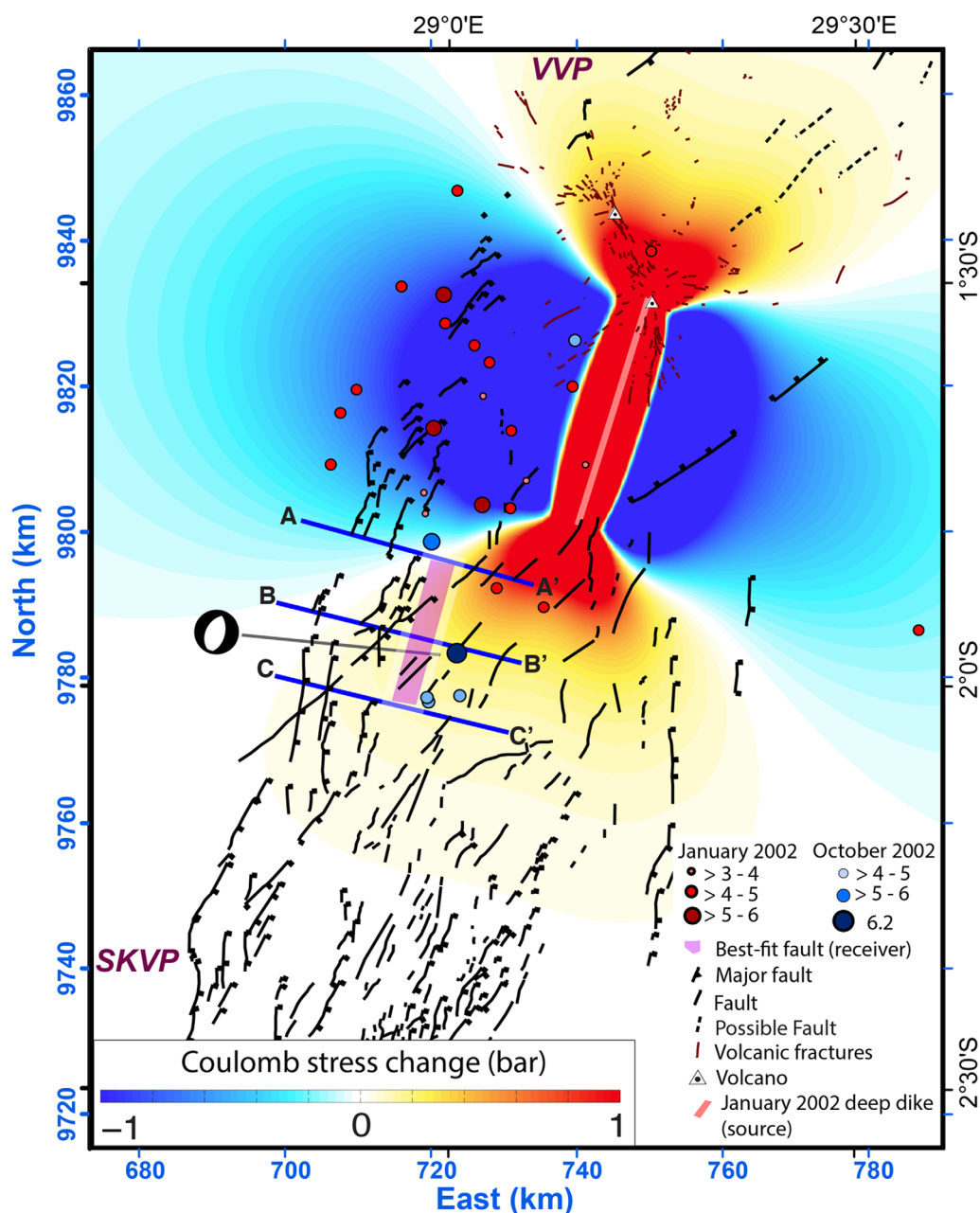


Figure 4. Mapped Coulomb stress changes (bars) induced by the 2002 deep dike intrusion (top is at ~ 3 km depth, height is ~ 6 km for a length of ~ 35 km, and a mean opening of ~ 0.72 m [Wauthier et al., 2012]) on receiver faults similar to the preferred best fit modeled fault (Table 2, Model 4). The Poisson's ratio and Young's modulus is 0.25 and 90 GPa, respectively. The coefficient of internal friction is 0.4, and the depth range is 3–8 km. Cross sections AA', BB', and CC' are shown in supplemental information Figure S8. Earthquakes for the period January to October 2002 are shown (source: NEIC).

Due to small amount of crustal stretching [Wood et al., 2015], we might expect the Kivu rift to be fault controlled. However, in the VVP, the intense magmatic activity identified in 1977 and 2002 is incompatible with a fault-controlled rift. Indeed, from the modeling of Wauthier et al. [2012], the 17 January 2002 Nyiragongo deformation sources account for a total geodetic moment of $\sim 1.3 \times 10^{19}$ Nm, mostly released by the deep dike beneath Goma and the Lake Kivu (Figure 2). The seismic moment for all January 2002 earthquakes (supplemental information Table S1) is only $\sim 3 \times 10^{17}$ Nm, 2 orders of magnitude smaller than the total January 2002 geodetic moment. If we consider all earthquakes in 2002 (including the October 2002 earthquakes), we obtain a seismic moment of $\sim 5 \times 10^{18}$ Nm, while the total geodetic moment, including the

January 2002 dikes and the October 2002 Kalehe faulting event, is $\sim 18 \times 10^{18}$ Nm. Therefore, $\sim 13 \times 10^{18}$ Nm or $\sim 72\%$ of the total $\sim 18 \times 10^{18}$ Nm moment release for the year 2002 in the Kivu basin is accounted for by aseismic processes. This is larger than for the Gelai dike event in 2007, in which $\sim 65\%$ of the total moment release is represented by aseismic processes [Calais *et al.*, 2008; Baer *et al.*, 2008; Biggs *et al.*, 2009]. However, in the Gelai case, a m_b 5.9 normal faulting event occurred before the dike intrusion. The ratio between seismic and total geodetic moment for the 2002 Nyiragongo-Kalehe sequence is similar to that of the 2005 Dabbahu rifting episode [Wright *et al.*, 2006], suggesting that magmatic intrusions release most of the extensional strain in both cases.

Discrepancy in strain accommodation in the Kivu basin is likely linked to proximity to major volcanic centers, where the proportion of tectonic fault-controlled deformation increases away from regions of active volcanism. Our stress change modeling also suggests that the along-rift variations in magmatic versus tectonic deformation is also modulated on a local scale by dike-induced faulting. Hence, the northern part of Lake Kivu could behave as a magma-assisted rift and the southern part as a fault-controlled rift. The VVP is volcanically active and participates in extension as active magma intrusion and underplating [Corti *et al.*, 2003a,b; Wood *et al.*, 2015]. Therefore, the area would accommodate the upper crustal extension by dikeing that triggers the seismic activity on the rift border. Likewise, the SKVP is not active and the southern part of Lake Kivu is accommodating extensional strain mainly with normal faulting [e.g., d'Oreye *et al.*, 2011]. This hypothesis is supported by longer-term indicators of deformation achieved in the structural analysis of Wood *et al.* [2015], and indicates that the along-rift variations in mechanism of deformation, and interaction between intrusion and induced faulting that we observe in the short term are indicative of long-term deformation patterns. The Kalehe area, in the center of Lake Kivu at the latitude of Idjwi Island, is located where the Kivu basin starts to transition structurally to a full graben further south, and could thus act as a structural boundary between two distinct local stress regimes.

Despite tectonic extension being the norm along most of the magma-poor Western Branch and the presence of large normal faults bounding the rift basins capable of $M7+$ earthquakes [Foster and Jackson, 1998], our new quantitative observations suggest localized areas, such as the northern Kivu basin, where magmatic extension dominates. The localized areas characterized by significant volcanism (and dominant magmatic extension) in the Western Branch correspond to regional transfer zones between major basins [e.g., Ebinger, 1989a; Corti *et al.*, 2003b] that probably contribute to rifting by feeding upper crustal dikes that could propagate laterally into the tips of rift basins [Muirhead *et al.*, 2015]. An active volcanic province could provide the short and long-term stress changes required to cause magma-assisted breakup of the continental lithosphere. Repeated dike intrusions induce magmatic heating, viscous weakening, and reduce the plate strength [Albaric *et al.*, 2014], providing a means to efficiently localize mechanical extension by ductile stretching and faulting relatively early during the rifting process [Buck, 2004]. Our observations suggest that a magmatic control on mechanical strain localization occurs in discrete parts of the Western Branch of the EAR, and may be critical in facilitating rupture in a largely magma-poor rift. The suggested interplay and causality between dikeing and normal faulting in a youthful cratonic continental rift like Kivu highlights the need for hybrid models to account for strain accommodation by magmatism, even during the early stages of rifting.

6. Conclusions

An integrated analysis of radar interferometry (InSAR), seismic and geological data, demonstrates that the Kalehe M_w 6.2 earthquake occurred due to normal-slip motion on a major preexisting east-dipping rift border fault. A Coulomb stress analysis suggests that dikeing events, such as the January 2002 Nyiragongo dike intrusion, could promote faulting on the western border faults of the rift in the central part of Lake Kivu. We thus interpret that dike-induced stress changes can cause moderate to large-magnitude earthquakes on major border faults during continental rifting. Continental crustal extension processes appear complex in the Lake Kivu basin, which seems to accommodate the rifting mostly with dike intrusions in its northern part and faulting in its southern part. This study suggests that dike intrusions play a major role in accommodating upper crustal extension in this part of the EARS, which is often considered as a magma-poor rift.

Acknowledgments

The interferograms were processed using ROI-PAC software and unwrapped with SNAPHU. The authors thank Nicolas d'Oreye, Valérie Cayol, François Kervyn, and Cindy Ebinger for useful discussions. The authors also thank M. Poland (USGS) for providing the RADARSAT-1 data and Erin DiMaggio for corrections of an earlier version of this manuscript. Benoît Smets is supported by the National Research Fund of Luxembourg (AFR PhD grant 3221321), the GeoRisCA Project (Belgian Science Policy Office, SSD Program, Contract SD/RI/02A), and the Vi-X Project (Belgian Science Policy Office, STEREO II Program, Contract SR/00/150; FNR Luxembourg, INTER Program; DLR, grant NTL_INSA0525). Derek Keir acknowledges support from Natural Environment Research Council grant NE/L013932/1. The facilities of IRIS Data Services, and specifically the IRIS Data Management Center, were used for access to waveforms, related metadata, and/or derived products from station MBAR used in this study. IRIS Data Services are funded through the Seismological Facilities for the Advancement of Geoscience and EarthScope (SAGE) Proposal of the National Science Foundation under Cooperative Agreement EAR-1261681. Finally, the authors are grateful to the Editor-in-Chief Thorsten Becker as well as to two anonymous reviewers for their thoughtful comments and suggestions.

References

- Albaric, J., J. Déverchère, J. Perrot, A. Jakovlev, and A. Deschamps (2014), Deep crustal earthquakes in North Tanzania, East Africa: Interplay between tectonic and magmatic processes in an incipient rift, *Geochem. Geophys. Geosyst.*, **15**, 374–394, doi:10.1002/2013GC005027.
- Baer, G., Y. Hamiel, G. Shamir, and R. Nof (2008), Evolution of a magma-driven earthquake swarm and triggering of the nearby Oldoinyo Lengai eruption, as resolved by InSAR, ground observations and elastic modeling, East African Rift, 2007, *Earth Planet. Sci. Lett.*, **272**(1), 339–352.
- Bellon, H., and A. Poulet (1980), Datations K-Ar de quelques laves du Rift-ouest de l'Afrique Centrale; implications sur l'évolution magmatique et structurale, *Geol. Rundsch.*, **69**(1), 49–62, doi:10.1007/BF01869023.
- Biggs, J., F. Amelung, N. Gommelen, T. H. Dixon, and S.-W. Kim (2009), InSAR observations of 2007 Tanzania rift episode reveal mixed fault and dyke extension in an immature continental rift, *Geophys. J. Int.*, **179**, 549–558.
- Biggs, J., E. Nissen, T. Craig, J. Jackson, and D. P. Robinson (2010), Breaking up the hanging wall of a rift-border fault: The 2009 Karonga earthquakes, Malawi, *Geophys. Res. Lett.*, **37**, L11305, doi:10.1029/2010GL043179.
- Biggs, J., M. Chivers, and M. C. Hutchinson (2013), Surface deformation and stress interactions during the 2007–2010 sequence of earthquake, dyke intrusion and eruption in northern Tanzania, *Geophys. J. Int.*, **195**(1), 16–26.
- Bilham, R., R. Bendick, K. Larson, P. Mohr, J. Braun, S. Tesfaye, and L. Asfaw (1999), Secular and tidal strain across the main Ethiopian rift, *Geophys. Res. Lett.*, **26**, 2792–2984.
- Buck, W. R. (2004), *Rheology and Deformation of the Lithosphere at Continental Margins*, edited by G. Karner et al., pp. 92–137, Columbia Univ. Press, USA.
- Calais, E., et al. (2008), Strain accommodation by slow slip and dyking in a youthful continental rift, East Africa, *Nature*, **456**(7223), 783–788.
- Chen, C. W., and H. A. Zebker (2001), Two-dimensional phase unwrapping with use of statistical models for cost functions in non linear optimization, *J. Opt. Soc. Am. A Opt. Image Sci.*, **18**, 338–351.
- Corti, G., M. Bonini, S. Conticelli, F. Innocenti, P. Manetti, and D. Sokoutis (2003a), Analogue modelling of continental extension: A review focused on the relations between the patterns of deformation and the presence of magma, *Earth Sci. Rev.*, **63**, 169–247.
- Corti, G., M. Bonini, F. Innocenti, S. Cloetingh, G. Mulugeta, D. Sokoutis, and P. Manetti (2003b), Rift-parallel magma migration and localisation of magmatic activity in transfer zones, *Acta Vulcanol.*, **14**, 17–26.
- Craig, T. J., J. A. Jackson, K. Priestley, and D. McKenzie (2011), Earthquake distribution patterns in Africa: Their relationship to variations in lithospheric and geological structure, and their rheological implications, *Geophys. J. Int.*, **185**, 403–434.
- Dawson, J., and P. Tregoning (2007), Uncertainty analysis of earthquake source parameters determined from InSAR: A simulation study, *J. Geophys. Res.*, **112**, B09406, doi:10.1029/2007JB005209.
- d'Oreye, N., et al. (2011), Source parameters of the 2008 Bukavu-Cyangugu earthquake estimated from InSAR and teleseismic data, *Geophys. J. Int.*, **184**, 934–948.
- Dziewonski, A. M., T.-A. Chou, and J. H. Woodhouse (1981), Determination of earthquake source parameters from waveform data for studies of global and regional seismicity, *J. Geophys. Res.*, **86**, 2825–2852.
- Ebinger, C. J. (1989a), Tectonic development of the Western Branch of the East African Rift System, *Geol. Soc. Am. Bull.*, **101**, 885–903.
- Ebinger, C. J. (1989b), Geometric and Kinematic development of border faults and accommodation zones, Kivu-Rusizi Rift, Africa, *Tectonics*, **8**, 117–133.
- Ebinger, C. J. (2005), Continental break-up: The East African perspective, *Astron. Geophys.*, **46**, 16–21.
- Ebinger, C. J., and T. Furman (2003), Geodynamical setting of the Virunga volcanic province, East Africa, in *Acta Vulcanologica, The January 2002 Eruption of Nyiragongo Volcano and the Socio-Economical Impact*, vol. 14(1-2) and 15(1-2), Ist. Editoriale Poligrafici Int., Pisa, Italy.
- Farr, T. G., et al. (2007), The shuttle radar topography mission, *Rev. Geophys.*, **45**, RG2004, doi:10.1029/2005RG000183.
- Foster, A. N., and J. A. Jackson (1998), Source parameters of large African earthquakes: Implications for crustal rheology and regional kinematics, *Geophys. J. Int.*, **134**, 422–448.
- Fukushima, Y., V. Cayol, and P. Durand (2005), Finding realistic dike models from interferometric synthetic aperture radar data: The February 2000 eruption at Piton de la Fournaise, *J. Geophys. Res.*, **110**, B03206, doi:10.1029/2004JB003268.
- Hayashi, Y., and Y. Morita (2003), An image of a magma intrusion process inferred from precise hypocentral migrations of the earthquake swarm east of the Izu Peninsula, *Geophys. J. Int.*, **153**(1), 159–174.
- Hellfrich, G. (1997), How good are routinely determined focal mechanisms? Empirical statistics based on a comparison of Harvard, USGS and ERI moment tensors, *Geophys. J. Int.*, **131**, 741–750.
- Kavotha, S. K., et al. (2003), Towards a more detailed seismic picture of the January 17th, 2002 Nyiragongo eruption, in *Acta Vulcanologica, The January 2002 Eruption of Nyiragongo Volcano and the Socio-Economical Impact*, vol. 14 (1-2) and vol. 15 (1-2), pp. 27–61, Ist. Editoriale Poligrafici Int., Pisa, Italy.
- Keir, D. (2014), Magmatism and deformation during continental breakup, *Astron. Geophys.*, **55**, (5), 18–22.
- Komorowski, J.-C., et al. (2003), The January 2002 flank eruption of Nyiragongo volcano (Democratic Republic of Congo): Chronology, evidence for a tectonic rift trigger, and impact of lava flows on the city of Goma, in *Acta Vulcanologica, The January 2002 Eruption of Nyiragongo Volcano and the Socio-Economical Impact*, vol. 14(1-2) and 15(1-2), pp. 27–62, Ist. Editoriale Poligrafici Int., Pisa, Italy.
- Koptev, A., E. Calais, E. Burov, S. Leroy, and T. Gerya (2015), Dual continental rift systems generated by plume-lithosphere interaction, *Nat. Geosci.*, **8**, 388–392.
- Lindenfeld, M., and G. Rümpler (2011), Detection of mantle earthquakes beneath the East African Rift, *Geophys. J. Int.*, **186**(1), 1–5.
- Mavonga, T. G. (2007), Some characteristics of aftershocks sequences of major earthquakes from 1994 to 2002 in the Kivu province, Western Rift Valley of Africa, *Tectonophysics*, **439**, 1–12.
- Mavonga, T. G. (2010), Crustal structure beneath two seismic broadband stations revealed from teleseismic P wave receiver function analysis in the Virunga volcanic area, Western Rift, *J. Afr. Earth Sci.*, **58**, 820–828, doi:10.1016/j.jafrearsci.2009.11.003.
- McKenzie, D. P. (1978), Some remarks on the development of sedimentary basins, *Earth Planet. Sci. Lett.*, **40**, 25–32.
- Midzi, V., and B. Manzunu (2014), The largest earthquakes in Sub-Saharan Africa, in *Extreme Natural Hazards, Disaster Risks and Societal Implications*, edited by A. Ismail-Sadeh et al., 413 pp., Cambridge Univ. Press, U. K.
- Morley, C. K. (1989), extension, detachments, and sedimentation in continental rifts (with particular reference to East Africa), *Tectonics*, **8**, 1175–1192.
- Muirhead, J., S. Kattenhorn, and N. Le Corvec (2015), Varying styles of magmatic strain accommodation across the East African Rift, *Geochem. Geophys. Geosyst.*, **16**, 2775–2795, doi:10.1002/2015GC005918.
- Nishimura, T., S. Ozawa, M. Murakami, T. Sagiya, T. Tada, M. Kaidzu, and M. Ukawa (2001), Crustal deformation caused by magma migration in the northern Izu Islands, Japan, *Geophys. Res. Lett.*, **28**, 3745–3748.

- Okada, Y. (1985), Surface deformation due to a shear and tensile faults in a half-space, *Bull. Seismol. Soc. Am.*, 75(4), 1135–1154.
- Parsons, T., and G. A. Thompson (1991), The role of magma overpressure in suppressing earthquakes and topography: Worldwide examples, *Science*, 253, 1399–1402.
- Passarelli, L., E. Rivalta, S. Cesca, and Y. Aoki (2015), Stress changes, focal mechanisms, and earthquake scaling laws for the 2000 dike at Miyakejima (Japan), *J. Geophys. Res. Solid Earth*, 120, 4130–4145, doi:10.1002/2014JB011504.
- Peeters, L. (1957), Contribution à l'étude de la genèse du lac Kivu, *Bull. Soc. Belge Etudes Géogr.*, 26, 155–168.
- Pottier, Y. (1978), *Première Eruption Historique du Nyiragongo et Manifestations Adventives Simultanees du Volcan Nyamulagira (Chaîne des Virunga - Kivu - Zaire: Dec. 76 - Juin 77)*, pp. 157–175, Musee R. Afr. Cent., Tervuren, Belgium.
- Poulet, A. (1976), Volcanologie du rift de l'Afrique centrale, le Nyamuragira dans les Virunga, Essai de magmatologie du rift, Ph.D. Thesis, University of Paris-Sud, Orsay, France.
- Poulet, A. (1977), Contribution à l'étude structurale de l'aire volcanique des virungas, rift de l'Afrique centrale, *Revue Géographie Physique et Géologie Dynamique*, 19, 115–124.
- Roberts, E. M., N. J. Stevens, P. M. O'Connor, P. H. G. M. Dirks, M. D. Gottfried, W. C. Clyde, R. A. Armstrong, A. I. S. Kemp, and S. Hemming (2012), Initiation of the Western Branch of the East African Rift coeval with the Eastern Branch, *Nat. Geosci.*, 5(4), 289–294.
- Rosen, P. A., S. Hensley, G. Peltzer, and M. Simons (2004), Updated repeat orbit interferometry package released, *Eos Trans. AGU*, 85, 47.
- Rosendhal, B. R. (1987), Architecture of continental rifts with special reference to East Africa, *Annu. Rev. Earth Planet. Sci.*, 15, 445–503.
- Ross, K. A., B. Smets, M. De Batist, M. Hilbe, M. Schmid, and F. S. Anselmetti (2014), Lake-level rise in the late Pleistocene and active sub-aquatic volcanism since the Holocene in Lake Kivu, East African Rift, *Geomorphology*, 221, 274–285.
- Sambridge, M. (1999a), Geophysical inversion with a neighbourhood algorithm – I. Searching a parameter space, *Geophys. J. Int.*, 138, 479–494.
- Sambridge, M. (1999b), Geophysical inversion with a neighbourhood algorithm—II. Appraising the ensemble, *Geophys. J. Int.*, 138, 727–746.
- Saria, E., E. Calais, D. S. Stamps, D. Delvaux, and C. J. H. Hartnady (2014), Present-day kinematics of the East African Rift, *J. Geophys. Res. Solid Earth*, 119, 3584–3600, doi:10.1002/2013JB010901.
- Shudofsky, G. (1985), Source mechanisms and focal depths of East African earthquakes using Rayleigh-wave inversion and body-wave modeling, *Geophys. J. R. Astron. Soc.*, 83, 563–614.
- Smets, B., C. Wauthier, and N. d'Oreye (2010), A new map of the lava flow field of Nyamulagira (D.R. Congo) from satellite imagery, *J. Afr. Earth Sci.*, 58, 778–786.
- Smets, B., M. Kervyn, N. d'Oreye, and F. Kervyn (2015), Spatio-temporal dynamics of eruptions in a youthful extensional setting: Insights from Nyamulagira Volcano (D.R. Congo), in the Western Branch of the East African Rift, *Earth Sci. Rev.*, 150, 305–328, doi:10.1016/j.earscirev.2015.08.008.
- Stamps, D. S., E. Calais, E. Saria, C. Hartnady, J.-M. Nocquet, C. J. Ebinger, and R. M. Fernandes (2008), A kinematic model for the East African Rift, *Geophys. Res. Lett.*, 35, L05304, doi:10.1029/2007GL032781.
- Tazieff, H. (1977), An exceptional eruption: Mt. Nyiragongo, January 10th, 1977, *Bull. Volcanol.*, 40(3), 1–12.
- Toda, S., R. S. Stein, and T. Sagiya (2002), Evidence from the A.D. 200 Izu Islands earthquake swarm that stressing rate governs seismicity, *Nature*, 419, 58–61.
- Toda, S., R. S. Stein, V. Sevilgen, and J. Lin (2011), Coulomb 3.3 Graphic-rich deformation and stress-change software for earthquake, tectonic, and volcano research and teaching—User guide, *U.S. Geol. Surv. Open File Rep.*, 2011-1060, 63 p.
- Villeneuve, M. (1980), La structure du Rift Africain dans la Région du Lac Kivu (Zaire oriental), *Bull. Volcanol.*, 43(3), 541–551.
- Wafula, D. M., et al. (2007), Natural disasters and hazards in the Lake Kivu basin, western rift valley of Africa, *IUGG Proc.*, 32 pp.
- Walter, T. R., and F. Amelung (2006), Volcano-earthquake interaction at Mauna Loa volcano, Hawaii, *J. Geophys. Res.*, 111, B05204, doi:10.1029/2005JB003861.
- Wauthier, C., V. Cayol, F. Kervyn, and N. d'Oreye (2012), Magma sources involved in the 2002 Nyiragongo eruption, as inferred from an InSAR analysis, *J. Geophys. Res.*, 117, B05411, doi:10.1029/2011JB008257.
- Wauthier, C., D. C. Roman, and M. P. Poland (2013), Moderate-magnitude earthquakes induced by magma reservoir inflation at Kilauea Volcano, Hawai'i, *Geophys. Res. Lett.*, 40, 5366–5370, doi:10.1002/2013GL058082.
- Wells, D. L., and K. J. Coppersmith (1994), New empirical relationships among magnitude, rupture length, rupture width, rupture area, and surface displacement, *Bull. Seismol. Soc. Am.*, 84(4), 974–1002.
- Wong, H.-K., and R. P. Von Herzen (1974), A geophysical study of Lake Kivu, East Africa, *Geophys. J. R. Astron. Soc.*, 37, 371–389.
- Wood, D. A., H. J. Zal, C. A. Scholz, C. J. Ebinger, and I. Nizere (2015), Evolution of the Kivu Rift, East Africa: Interplay between tectonics, sedimentation, and magmatism, *Basin Res.*, 1–14, doi:10.1111/bre.12143, in press.
- Wright, R., M. Blackett, and C. Hill-Butler (2015), Some observations regarding the thermal flux from Earth's erupting volcanoes for the period of 2000 to 2014, *Geophys. Res. Lett.*, 42, 282–289, doi:10.1002/2014GL061997.
- Wright, T. J., C. Ebinger, J. Biggs, A. Ayele, G. Yirgu, D. Keir, and A. Stork (2006), Magma-maintained rift segmentation at continental rupture in the 2005 Afar dyking episode, *Nature*, 442(7100), 291–294.
- Wright, T. J., et al. (2012), Geophysical constraints on the dynamics of spreading centres from rifting episodes on land, *Nat. Geosci.*, 5, 242–250.
- Yang, Z., and W.-P. Chen (2010), Earthquakes along the East African Rift System: A multiscale, system-wide perspective, *J. Geophys. Res.*, 115, B12309, doi:10.1029/2009JB006779.
- Yokoyama, I. (2001), The largest magnitudes of earthquakes associated with some historical volcanic eruptions and their volcanological significance, *Ann. Geophys.*, 44(5–6).
- Zana, N., and H. Hamaguchi (1978), Some characteristics of aftershocks sequences in the Western Rift Valley of Africa, *Geophysics*, 25(2), 55–72.